Acta Cryst. (1968). A24, 657

Electron Diffraction of U_4O_9

BY H. BLANK AND C. RONCHI

Institut für Transurane, Euratom, 75 Karlsruhe, Postfach 2266, Germany

(*Received* 11 *March* 1968)

Thin foils of U_4O_9 prepared from bulk single crystals of UO_2 were investigated at 20 °C and between 300 °C and 1000 °C in the electron microscope. At 20 °C the complete reciprocal lattice of U_4O_9 has been established. Between about 550° and 700 °C an order–partial disorder transformation has been found in most of the specimens investigated. This leads to a modified U–O phase diagram but at present it is not known if this new diagram or the old one represents metastable phase relations. Crystallographic relations between the low temperature phase and the partly disordered high-temperature phase of U_4O_{9-y} have been deduced.

1. Introduction

The behaviour of excess oxygen in the fluorite structure of UO_2 is complicated and is still not well understood in spite of the numerous papers which have appeared on this subject. The properties of $UO_{2\cdot25}$ and U_4O_9 are of special interest since at this composition the excess oxygen amounts to one additional oxygen atom per unit cell of UO_2 and is arranged in a superlattice which can be disordered at higher temperatures.

Important contributions to the present knowledge concerning oxygen in UO_{2+x} and U_4O_9 came from X-ray diffraction (Grønvold, 1955; Belbeoch, Piekarski & Perio, 1961; Belbeoch, Laredo & Perio, 1964; Naito, Ishii, Hamaguchi & Oshima, 1967; Belbeoch, Boivineau & Perio, 1967), neutron diffraction (Willis, 1963, 1964) and vapour pressure and E.M.F. measurements. [For a review and collection of data see Markin & Roberts (1962).] The interpretation of magnetic susceptibility investigations (Gotoo, Nomura & Naito, 1965; Nasu, 1966; Leask, Roberts, Walter & Wolf, 1963) unfortunately is not clear because the exact oxygen positions are lacking and therefore the symmetry of the crystal field is unknown.

So far all structural investigations on single-crystal and powder specimens of U_4O_9 have been performed with either X-rays or neutrons.* Both methods have certain limitations: X-rays give high resolution but have low scattering power for oxygen; with neutron diffraction the exact reverse is the case, the scattering properties for oxygen being good while high resolution of the many superlattice reflexions is lacking (Andresen, 1959). In spite of this last difficulty the most detailed progress for the location of the positions of oxygen in UO_2, UO_{2+x} and U_4O_9 has come from this technique, though for U_4O_9 only an analysis of the intensities of the basic UO_2 reflexions has been published (Willis, 1964).

Because of these experimental difficulties a first attempt was made to investigate U_4O_9, prepared from bulk material, by electron diffraction. Again there are experimental limitations; this time the intensities are not observable with any precision but as will be shown in this paper, several new experimental facts have been found by this method. We shall be concerned with the behaviour of U_4O_9 at room temperature and at temperatures between about 300 and 1000 °C and sometimes up to 1100 °C, disregarding the transformation at 60–80 °C which obviously only changes the intensity of the superlattice spots but does not affect the symmetry of the structure (Naito, Ishii, Hamaguchi & Oshima, 1967) though there is a noticeable change in lattice parameter (Grønvold, 1955; Naito, Ishii, Hamaguchi & Oshima, 1967; Belbeoch, Boivineau & Perio, 1967; Ferguson & Street, 1963).

Both X-ray and neutron diffraction have led to the conclusion that U_4O_9 has space group $I\bar{4}3d$ with a lattice parameter nearly four times that of UO_2, but no complete reciprocal lattice of U_4O_9 has been published. The model for the oxygen positions proposed by Belbeoch, Piekarski & Perio (1961) on the basis of X-ray evidence seems difficult to reconcile with the neutron diffraction results of Willis (1964) who showed that an excess oxygen ion does not occupy the centre of an octahedral hole of the fluorite structure but is attracted by two uranium ions and therefore pushes two oxygen ions off their normal lattice sites into interstitial positions.

Because of the complexity of this structure it seems worth while to collect and compare as many crystallographic and physical data as possible in order to get a sound basis for a reliable model. This paper gives a contribution to this experimental basis, though this basis seems to be a complicated one. In fact, the more experimental data become available on U_4O_9 (Naito, Ishii, Hamaguchi & Oshima, 1967; Belbeoch, Boivineau & Perio, 1967) the more complex are the aspects of this phase revealed.

* We shall not deal here with thin film effects as found by Steeb (Steeb, 1961; Steeb & Mitsch, 1965) by electron diffraction.

2. Experimental procedure

Large single crystals of UO_2* were cut into thin discs fitting into a slightly modified specimen holder of an Elmiskop IA. The planes of the platelets were chosen near a (100) or (110) plane. The discs were either equilibrated with U_3O_8 for 6 to 60 hours after sealing in silica tubes or oxidized under an air pressure of 10^{-2} torr at 900 °C for 5 hours to U_4O_9. The specimens were then thinned in hot orthophosphoric acid for transmission electron microscopy. Several specimens were investigated in the electron microscope at room temperature.

Eight specimens were mounted into the normal heating stage of the Elmiskop and observed at temperatures up to about 1000 °C. In this case no tilting was possible. The precision of the temperature measurement certainly was not better than ±40 °C. In the temperature range between 400 °C and 800 °C specimens were kept between half an hour and 3 hours at temperature and diffractions were taken at regular time intervals in order to see if changes in the diffraction patterns occurred. The time to reach thermal equilibrium after an increase in temperature by 50 to 100 °C was about 5 minutes as indicated by the termination of the thermal shift of the specimen. In this way the specimens were cycled between 4 and 10 times between room temperature and 1000 °C.

In some samples mounted in the normal specimen holder certain areas were heated quickly with the electron beam below the melting point and then quenched very rapidly by turning off the beam. By this procedure regions of U_4O_9 could be produced which showed at room temperature the same or very similar diffraction patterns as were found above about 600 °C in the heating stage. This confirms that it is possible to retain a high temperature phase of U_4O_9 at 20 °C by quenching, as shown already by X-ray diffraction (Belbeoch, Laredo & Perio, 1964). All specimens were observed at 100 kV accelerating potential. In the following we shall not go into the details observed on the electron micrographs but shall mainly be concerned with the diffraction patterns.

3. Experimental results

3.1. *Diffraction patterns at room temperature*

Figs. 1 to 4 give examples of room temperature diffraction patterns of U_4O_9. The details are explained in the caption of each figure. Closer inspection of the negatives reveals some features more clearly than can be observed on the positive prints shown here. The following facts can be stated:

(i) In Fig. 1 the square pattern of extremely intense big spots is due to the basic UO_2 lattice. In the notation of the big U_4O_9 unit cell with $a=4a_0$ the sides of the squares around the origin are given by the reciprocal lattice vectors $\mathbf{g}=\pm[800]$ and $\pm[080]$. In the notation of the basic UO_2 lattice these vectors would be called $\pm[200]$ and $\pm[020]$. We shall use only the notation of the big U_4O_9 cell if not otherwise stated.

(ii) The pattern of superstructure points in the first order unit cell of the reciprocal lattice is repeated with the same relative intensity distribution in all higher order cells. Superlattice spots in the range

$$2 \text{ or } 6 \leq (h^2+k^2+l^2) \lesssim 2000$$

have been observed.

(iii) From visual inspection the intensities of the superlattice spots have been divided into four classes: strong, medium, weak, very weak. The 'very weak' spots are absent or partly absent in some diffraction patterns. In Table 1 the main types of spots representative of each class have been listed; this list is not exhaustive.

Table 1. *Classification of superlattice spots according to their intensities*

Strong	(*a*)	{130} {150} {240}
	(*b*)	{112}
Medium	(*c*)	{220} {660} {260}
Weak	(*d*)	{400} {440}
Very weak	(*e*)	{110} {330} {350} {550} {770} {*hh*0} $h=2n+1$
	(*f*)	{200} {600} {*h*00} $h=2(2n+1)$

In Fig. 5 the unit cell of the reciprocal lattice of U_4O_9 as deduced from Figs. 1 to 4 is presented omitting the spots of the class 'very weak' by making use of the cubic symmetry of the structure. See also Table 2.

(iv) Each reflexion of the basic UO_2 lattice is surrounded by a polyhedron whose corners are represented by 24 strong superlattice reflexions of type

$$\mathbf{g}+\{112\}$$

where $\mathbf{g}$ is a reciprocal lattice vector of the basic UO_2 lattice (Fig. 9).

(v) Because of the many difficulties involved it is not possible to give reliable figures for the absolute intensities of either UO_2 or superlattice spots.

(vi) Two specimens gave a diffraction pattern which has a symmetry different from the patterns of Figs. 1 to 5. The reason for this difference is unknown. These specimens have been prepared in completely the same way as the others from the same stock of starting material. Their structure does not belong to the same space group as the normal U_4O_9. The specimens kept their particular structure also after heating and recooling. Details on this structure will be reported elsewhere.

3.2. *High temperature diffraction patterns and the order–partial disorder transformation*

3.2.1. *General behaviour*

When the specimens are heated above about 450 °C, profound and reversible changes in the diffraction pat-

* Supplied by NUKEM, Hanau, Germany.

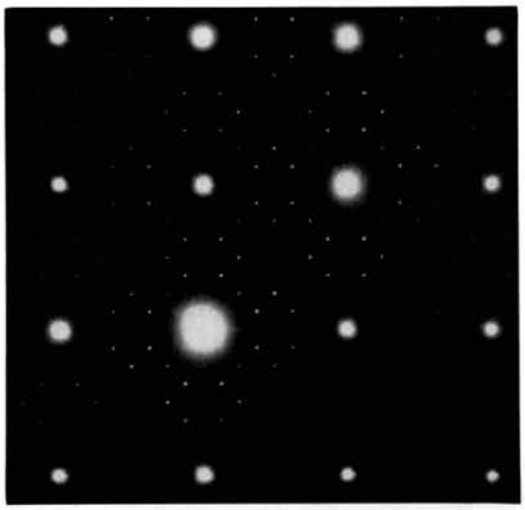

Fig. 1. Diffraction pattern with plane of the foil close to (001) at 20 °C. Note the group of six 'strong' superlattice reflexions of types 130, $\bar{1}30$, 240, $\bar{2}40$, 150, $\bar{1}50$ between each two extremely strong basic reflexions on the directions ⟨800⟩. 'Weak' reflections of type 400 and 440 are recognized easily. 'Very weak' reflexions of types 200, 110, 330, 550, 350, and 530 can also be found.

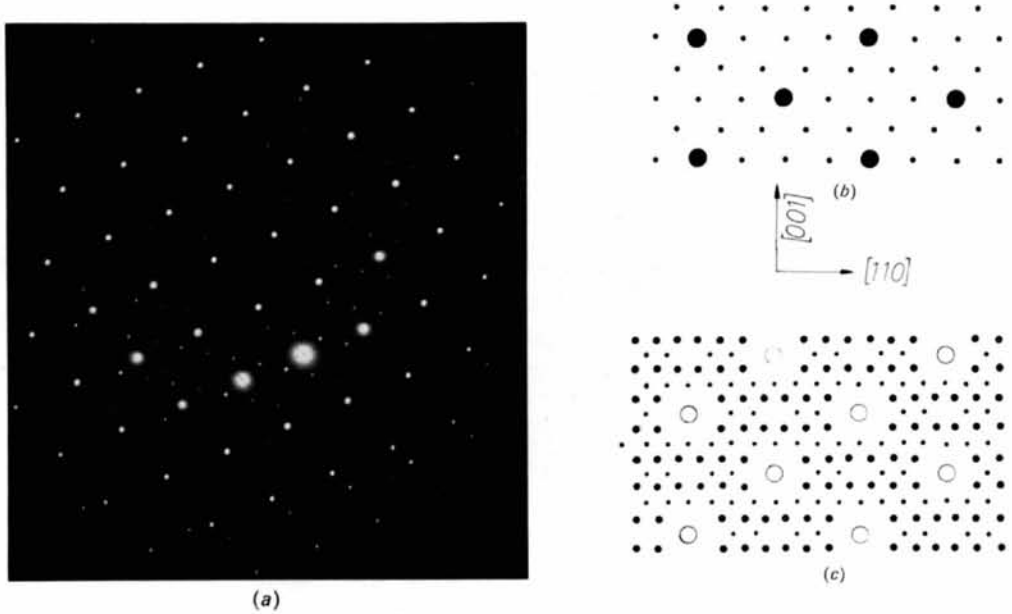

(a)

Fig. 2. (*a*) Diffraction pattern of U_4O_9 with the plane of the foil close to ($\bar{1}10$), but tilted slightly about an axis [311], at 20 °C. In the ($\bar{1}10$) plane each basic UO_2 reflexion is surrounded by four strong superlattice reflexions of type {112}. In the bottom right part of the picture, traces of the next plane parallel to the ($\bar{1}10$) plane of the reciprocal lattice can be seen. (*b*) Drawing of the complete reciprocal lattice around the origin and top left part of Fig. 2(*a*), ($\bar{1}10$) plane of the reciprocal lattice of U_4O_9. Heavy full circles are basic UO_2 reflexions. (*c*) Next two parallel reciprocal lattice planes to the one shown in Fig. 2(*b*). They are at a distance $[\bar{1}10]$ and $\frac{1}{2}[\bar{1}10]$ from the origin and do not contain basic UO_2 reflexions but often these can still be observed (open circles). In the bottom left part of Fig. 2(*a*) mainly those spots can be observed which are marked heavier in the drawing.

[*To face p.* 658

Fig. 3. Diffraction pattern of another specimen with ($\bar{1}10$) orientation at 20°C. Here the two patterns of Fig. 2(*b*) and (*c*) are superposed.

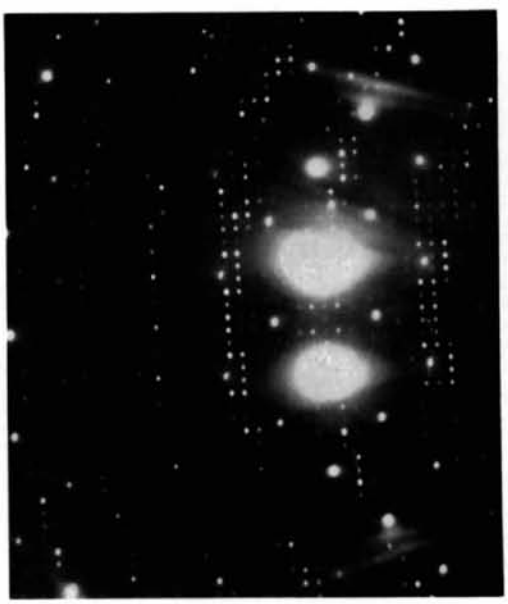

Fig. 4. Diffraction pattern of a specimen with the plane of the foil (001) tilted about a [$\bar{1}10$] direction. From diffraction patterns of this type the complete reciprocal lattice as shown in Fig. 5 has been constructed.

terns usually began to appear. On cooling back to room temperature, the original U_4O_9 superstructure is restored. By quenching, the high temperature state can be fixed at 20°C with some slight modifications. Yet one of the eight specimens investigated did not show this transformation but kept its low temperature superlattice reflexions up to 1000°C.

For the following reasons it was not possible to establish an exact temperature of transformation.

(i) As mentioned before, the temperature of the specimen is known only with low precision, because it cannot be measured directly.

(ii) Usually a specimen was cycled several times in steps of 50° to 100° between 20° and 1000°C. Each temperature cycle caused some loss of oxygen and at the same time reduced the temperature T_c around which the transformation takes place from as high as 800°C down to about 500°C. One specimen did not show any transformation at all up to 1000°C.

(iii) From the prolonged heat treatments around T_c it is concluded that under the conditions used there existed no exact temperature of transition, but the transformation took place in a temperature interval of about $\Delta T \sim 60$°C in times up to about 4 hours. It is not known if one could reduce this value of ΔT by sensibly extending the holding times at the temperatures around $T_c \pm \Delta T/2$.

(iv) It seems possible that the transformation is favoured by the action of the electron beam, either indirectly by local heating of the specimen or directly by elastic high angle scattering of 100 kV electrons by the oxygen ions. This is suggested by the fact that an area of the specimen which had been under observation several times at a given temperature showed the transformation, whereas another area, not being exposed to the beam before, had not yet transformed to the same extent, but did so during observations.

It can be inferred from the following facts that a reduction of U_4O_9 takes place in the electron microscope at higher temperatures. The specimens are kept in the electron microscope at an air pressure of about 5×10^{-7} to 10^{-4} torr. The equilibrium oxygen pressure for U_4O_9 between 600° and 1000°C is about 10^{-7} and 6×10^{-3} torr respectively (Markin & Roberts, 1962). This means at the highest temperatures used in this investigation, the U_4O_9 is subject to slightly reducing conditions. The reduction of U_4O_9 to U_4O_{9-y} could not be observed directly, only the lowering of T_c may be taken as an indication. This process certainly is slow.

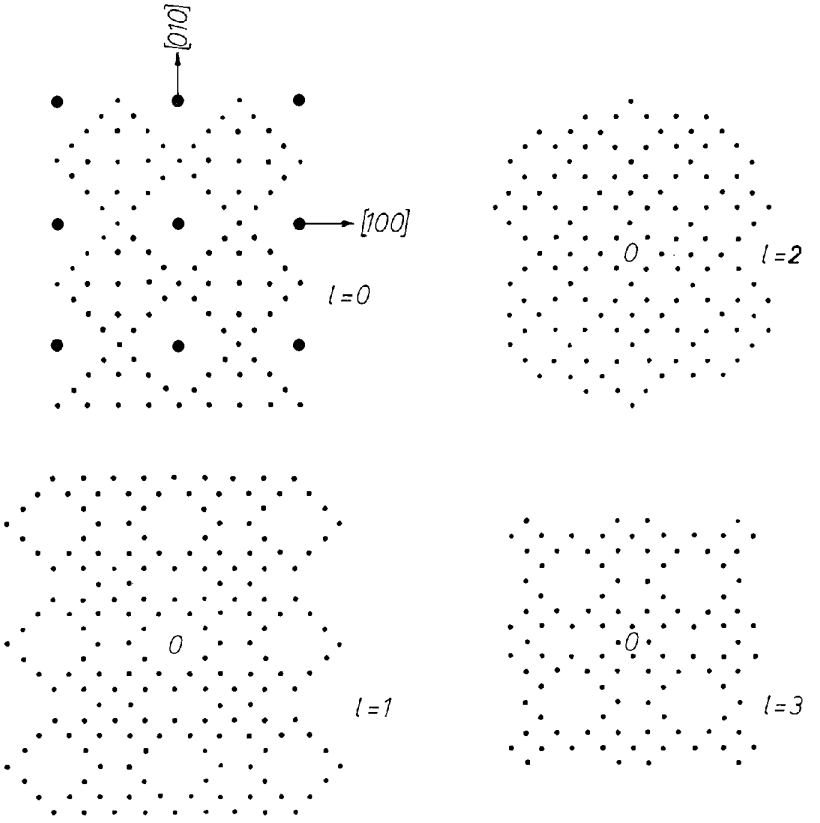

Fig. 5. Reciprocal lattice of U_4O_9. Top left shows the cube plane containing the origin; see diffraction pattern Fig. 1. The next three parallel planes with $l=1$, 2 and 3 are given in the same orientation; the projection of the origin into these planes is indicated. The reciprocal lattice planes with $l=4$, 5, 6, 7 have the same pattern as the ones shown in this drawing, but their origin is displaced by a vector [440]. The indices of the points are given in Table 2.

But as soon as the phase boundary U_4O_{9-y}/UO_{2+x} is crossed in the region under observation precipitates of UO_{2+x} appear in the matrix of U_4O_{9-y}. These can easily be detected on the electron optical images.

Once precipitates of UO_{2+x} have been nucleated, one gets the impression that reduction is accelerated by moving the interface UO_{2+x}/U_4O_{9-y} to the U_4O_9 side. Single dislocations and small angle boundaries may inhibit this reduction process, that is, these lattice defects block the movement of the UO_{2+x}/U_4O_{9-y} interface. Reoxidation of the single-crystal specimens at temperatures below 800 °C has not been observed during times up to about 4 hours.

In conclusion we may suggest that for stoichiometric U_4O_9, the oxygen superlattice is rather stable and the temperature T_c is rather high. Yet as soon as this superlattice contains vacancies, the oxygen ions have gained sufficient freedom for disordering. Then just by thermal motion the fixed superlattice positions may relax and superlattice spots in the diffraction pattern are destroyed. The greater the value of y in the formula U_4O_{9-y}, the easier this relaxation may occur, that is, the lower is the temperature T_c. We shall now follow this process in more detail by regarding the diffraction pattern of U_4O_{9-y} above the temperature T_c.

3.2.2. *The high temperature diffraction patterns*

Examples of diffraction patterns above the temperature T_c are shown in Figs. 6 to 8. These plates were taken at 700° and 950 °C with the exception of Fig. 8 showing a quenched disordered U_4O_9 pattern at room temperature. Patterns like Figs. 6 and 7 persist up to at least 1000 °C and change back to those of Figs. 1 to 4 on cooling below T_c. Sometimes also residual superlattice spots persist at $T > T_c$, as can be found in Fig. 7.

The main features of the transformation behaviour and of the high temperature diffraction patterns can be described as follows in contrast to the low temperature diffractions.

(i) Most of the numerous superstructure reflexions existing below T_c disappear on heating around T_c.

(ii) In the place of the strong $\mathbf{g}+\{112\}$ type low temperature spots there appear diffuse streak-like satellites to those reflexions $\mathbf{g}$ which are adjacent to the most intense basic UO_2 reflexions (Figs. 6, 7 and 8). Sometimes traces of the low temperature spots can still be seen in these satellites at $T > T_c$.

(iii) Besides the residual $\mathbf{g}+\{112\}$ spots, superlattice reflexions of type {400} and {440} and their higher orders are the most persistent reflexions at $T > T_c$. Below T_c the {400} and {440} spots had to be classified as 'weak' (Table 1). This means that these latter superlattice spots have gained intensity by the transformation (Fig. 7), whereas the rest have been destroyed. But they are not always preserved (Fig. 6) whereas the streak-like satellites are present in any case.

(iv) The basic UO_2 reflexions without satellites are surrounded by a rather symmetrical diffuse intensity distribution. Often bands of diffuse intensity are connecting the basic UO_2 reflexions in ⟨110⟩ directions above T_c. Kikuchi bands, which are also present (Figs. 6 and 7), should not be confounded with these diffuse intensities.

(v) If the high temperature state is quenched to 20 °C, much of the diffuse intensity, distributed in reciprocal space outside the streaks and the basic UO_2 reflexions at high temperature, is reduced and the diffuse streak-like satellites become sharp narrow lines of the same width as the UO_2 reflexions as shown in Fig. 8.

(vi) At temperatures $T \sim 1100$ °C the streaks are becoming fainter, but owing to the limitations of the furnace it was not possible to increase the temperature further and make the streaks disappear completely.

From these observations it follows that in the first place the diffuse streak-like satellites represent the difference between UO_{2+x} and the U_4O_9 phase in the temperature range $T_c \lesssim T \lesssim 1130$ °C. But also the reflexions of type 400 and 440 must play some role in the transformation taking place around T_c.

The geometry of the streaks should give indications on the transformation and on the high temperature structure of U_4O_9. It can best be studied by comparing their positions in the diffraction patterns with (110) and approximate (001) orientation, with the 24 {112} superlattice reflexions as represented in Fig. 9. This drawing shows that the streak-like satellites have been produced by smearing out the intensity of groups of three {112}-type low temperature superlattice spots into the triangular area between them as shown by the hatching in Fig. 9(*a*) and (*b*).

The geometry of the streaks in Fig. 7 agrees with this explanation since the plane of the diffraction pattern is a (001) plane tilted approximately 8° about both its [100] and [010] axes. This can be shown by relating Fig. 9(*a*) to Fig. 7. One has to place the centre O of a polyhedron like that of Fig. 9(*a*) in each basic UO_2 reflexion which shows satellites. The Ewald sphere then cuts the sides of these polyhedra facing the origin between $l=0$ and $l=1$ and the opposite sides between $l=1$ and $l=2$ [Fig. 9(*c*)], because of the orientation of the crystal foil. Consequently the satellites cannot be revealed at the sides of the basic UO_2 reflexions facing the origin, but only at the opposite sides.

This gives a cut through an equivalent triangular-like shaped region as in Fig. 6, but now at right angles to that of Fig. 6. This proves that the streaks are in fact triangular disc shaped volumes in reciprocal space and a diffraction pattern with orientation (001) exactly parallel to the electron beam will not reveal them near the origin.

The normals of the discs point to the next 444 type reflexions (Fig. 6), and the distance of the centre of gravity of the disc from its basic UO_2 reflexion to

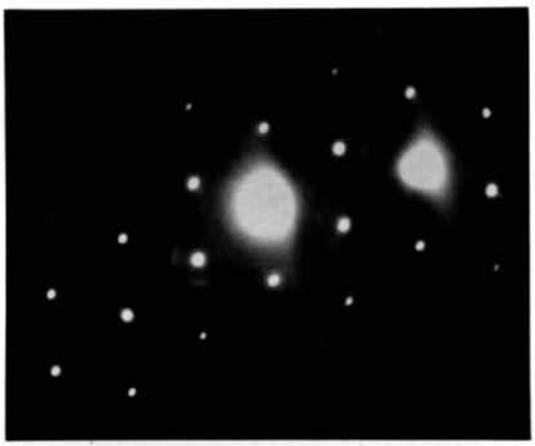

Fig. 6. Diffraction pattern with orientation of the specimen near ($\bar{1}10$) at 720 °C. All superlattice spots have disappeared; only faint streak like satellites can be found around some basic UO_2 reflexions.

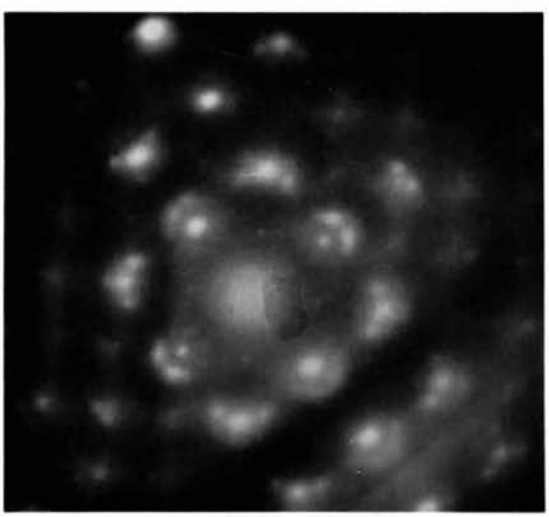

Fig. 7. Diffraction pattern of U_4O_9 at 950 °C with the plane of the foil near (001). Besides the streak like satellites superlattice spots of type {440} can be recognized.

[*To face p.* 660

Fig. 8. High temperature diffraction pattern of U_4O_9 quenched to 20 °C. The streaks now have the same width as the other reflexions. Orientation of the foil: (001) plane tilted about the [010] axis.

which it is attached is found to be about $\frac{1}{3}$[444] (Fig. 6). This is exactly what is to be expected on the basis of Fig. 9(*c*). The thickness of the discs at 700 °C is of the order of 0·02 Å^{-1}, but as mentioned above, it is reduced to a very small value if this structure is quenched to 20 °C.

4. Discussion

4.1. *Comparison of room temperature diffraction with X-ray results*

In order to compare the electron diffraction patterns with the work of Belbeoch, Piekarski & Perio (1961), we should first decide on the origin of the 'very weak' spots mentioned in Table 1 and § 3.1.

A priori three possibilities exist:

(*a*) Thin film effects, that is the relrod of two parallel next neighbour planes of the reciprocal lattice appear on the same diffraction pattern. This effect is strongly dependent on the orientation since the distance between consecutive (110) planes is only $2^{-1/2}$ with respect to corresponding (001) planes and still less for planes with higher indices.

(*b*) Double diffraction; this means that the strongest superlattice spots act as primary beams and produce the very weak spots.

(*c*) True diffraction spots.

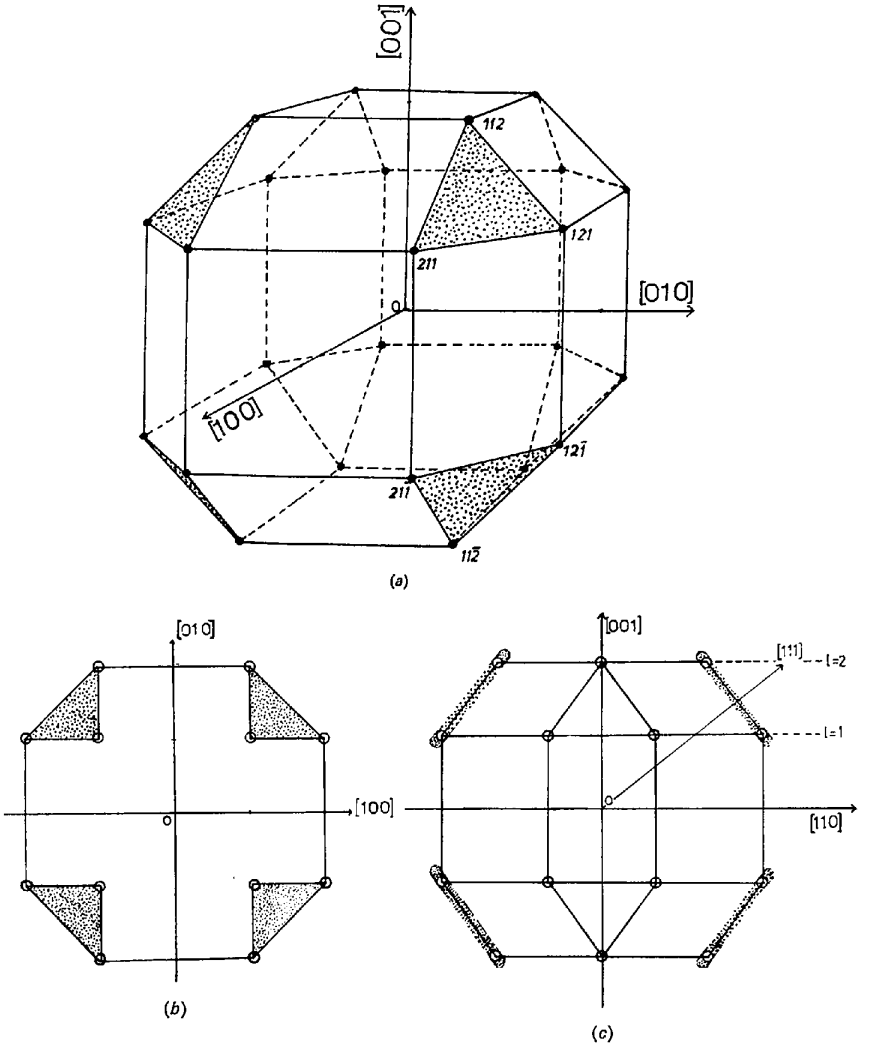

Fig. 9. (*a*) The polyhedron defined by the 24 superlattice spots of type {112} at room temperature. Its center *O* may be any basic UO_2 reflexion of the U_4O_9 reciprocal lattice. There are eight groups of three superlattice spots defining the eight triangles of which four are marked by small points in the drawing. At $T > T_c$ the intensity of each group of three spots is distributed evenly over and around the area of the triangles as indicated in Fig. 9(*c*). (*b*) Projection of Fig. 9(*a*) onto the (001) plane. (*c*) Projection of Fig. 9(*a*) onto the ($\bar{1}$10) plane. The distribution of intensity around the marked triangles of (*a*) and (*b*) at $T > T_c$ is indicated. Because of this geometry, the streaks cannot be observed in foils orientated exactly with [001] parallel to the beam. The distance of the streaks from the center *O* is given by relation (2) of § 4·4.

(i) *Diffraction patterns with* (001) *orientation* (Fig. 1). The first possibility – thin film effects – may be discarded for the following reasons. The extinction distance t_g of superlattice reflexions is always much larger than that of normal lattice reflexions. The maxima of intensity I along a relrod according to the kinematical approximation of electron diffraction which applies here are given by (see *e.g.* Amelinckx, 1964; Hirsch, 1965):

$$I/I_0 \simeq \frac{1}{1+W^2} \quad W = st_g \, .$$

Taking $W \simeq 4$ as a value which still gives an observable intensity results in a distance s of the ideal reciprocal lattice point from the surface of the Ewald sphere which is much smaller than the distance between planes $l=0$ and $l=1$ in Fig. 5. This means, in spite of the rather crowded reciprocal lattice of U_4O_9 its parallel (001) type planes are all well separated for 100 keV electrons. Furthermore the very weak spots of Fig. 1 could only originate in a plane with $l=2$ (Fig. 5), which is even less probable under these conditions. On the other hand the 'very weak' spots may easily be explained by double diffraction.

(ii) *Diffraction patterns with* (110) *orientation or close to it* [Figs. 2(*a*) and 3]. In Fig. 2(*a*) no extra 'very weak' spots were observed on the negative. The plane of the pattern is not an exact $(\bar{1}10)$ plane but is rotated somewhat about a vector $g=\langle 44-12\rangle$ and one can see a zone where the Ewald sphere has cut the next parallel planes of the reciprocal lattice with distance $2^{-1/2}$ and $\sqrt{2}$ from the origin. Both planes are shown in Fig. 2(*b*) and (*c*) as drawings, constructed from Fig. 5. Fig. 3 on the other hand can be identified as a superposition of the two patterns of Fig. 2(*b*) and (*c*). In some cases a few 'very weak' points have been observed close to the basic UO_2 reflexions in diffraction patterns similar to Fig. 3 in the areas which should be free of superlattice reflexions. But it is difficult to decide if they were due to double diffraction or real diffraction spots. On the other hand the very weak spots seen in Fig. 1 have never been found in crystal foils with orientation (110). In conclusion we can assume with some reason that the spots of type 'very weak' are not true diffraction spots.

The following discussion will be limited to the superlattice reflexion in the unit cell of the reciprocal lattice only, because as mentioned in § 3.1, in all higher order reflexions the intensity distribution of this unit cell is repeated.

The unit cell contains 186 superlattice reflexions which are produced by the permutation of the index triples given in Table 2. The superlattice reflexions can be divided into the 5 groups shown in Table 2. As far as possible for each group the intensities estimated visually from the photographic plates are given.

Nearly all superlattice reflexions which have been classified 'medium' and 'weak' in Tables 1 and 2 are missing from the X-ray patterns of Belbeoch, Piekarski & Perio (1961). The strongest X-ray superlattice reflexions are given by the $\mathbf{g}+\{112\}$ type reflexions of Table 2 in agreement with electron diffraction.

Table 2. *The complete set of superlattice reflexions of the unit reciprocal lattice cell of* U_4O_9 *of space group* $I\bar{4}3d$

For comparison with *International Tables* also the general rule for each group of reflections is given. Reflexions mentioned by Andresen (1959) have been marked by an asterisk.

w	*s*	*w*	*w*
004	204*	220	224
044	604*	260	264
		660	664
$8n$	$4n+2$	$4n+2$	
$4n$	$8n$	$4n+2$	
$8n+4$	$8n+4$	$4n$	
s	*s*	*s*	
112	116	130	134
332	336	150*	154
552*	556	370	374
772	776	570	574
172	176		
352	356		
	m		
132	136*		
152	156		
372	376		
572	576		
$2n+1$		$8n\pm1$	
$2n+1$		$8n\pm3$	
$4n+2$		$4n$	

s = strong, *m* = medium, *w* = weak.

We may state that all X-ray reflexions of Belbeoch, Piekarski & Perio (1961) are also present in the electron diffraction patterns but that electron diffraction gives more reflexions not found by X-rays. Especially it may be pointed out that superlattice reflexions exist also at small angles, strong reflexions of type {112} can be seen in Fig. 2(*a*) for instance, and furthermore reflexions of type $h00$ with $h=4(2n+1)$ exist, whereas Belbeoch *et al.* did not see these spots and concluded from this that a periodicity with $a_0/2$ along the cubic axes should be kept. Obviously this reasoning is not valid.

Unfortunately no list of superlattice reflexions due to neutron diffraction seems to have been published. Willis (1964) only mentions that he found amongst others one or two 'very weak' superlattice reflexions with $h_i=4n$ ($h_i=h,k,l$). This type of reflexion has been classified as 'weak' in Tables 1 and 2 but was observed here to be rather persistent during the transformation near 550 °C to 700 °C (see § 3.2.2). The superlattice reflexions found by Andresen (1959) with neutron diffraction have been noted with an asterisk in Table 2 as far as they agree with our results. In addition he has indexed his diagram with a reflexion 612 which does not belong to a body-centred structure and with the two reflexions 503 and 305 which

also do not exist in Table 2. The intensities of his reflexions indicated in Table 2 are in qualitative agreement with the electron diffraction results.

The limiting conditions for possible reflexions (Table 2) are in agreement with space group $I\bar{4}3d$ as determined first by Belbeoch, Piekarski & Perio (1961) and confirmed by Willis (1964). It is interesting to note that most of the superlattice extinctions are due to the subgroup 12(*a*), 12(*b*) of *International Tables* which concern only fixed positions without possible displacements.

4.2. *The oxygen positions in* U_4O_9 *proposed in the literature* (Belbeoch, Piekarski & Perio, 1961; Willis, 1964; Andresen, 1959; Kingery, 1965; Aronson & Belle, 1958)

Belbeoch, Piekarski & Perio (1961) were the first to propose a complete model of oxygen positions in U_4O_9. Even if this model was not to be retained in the future it was the first important step to attack the problem. The main conclusions from this model are:

(i) The 64 excess oxygen atoms are distributed rather heterogeneously in the big U_4O_9 cell; 48 of them are arranged in 12 groups of four. Each group forms a tetrahedron on next neighbour octahedral interstitial sites and gives a very high local density of oxygen. The remaining 16 oxygen atoms occupy isolated octahedral interstices halfway between these groups [positions 16(*d*)].* The distance D between two neighbouring groups is $D=a_0/2\langle 134\rangle=2{\cdot}505\ a_0$ and the diameter d of one tetrahedron is of the order of $d\sim a_0/\sqrt{2}=0{\cdot}706\ a_0$; a_0 is the lattice parameter of the small UO_2 subcell. Thus relatively large parts of the structure consist of stoichiometric UO_2 in the U_4O_9 cell according to this model.

(ii) The 12 tetrahedra of interstitial oxygen atoms occupy the positions 48(*e*) and these positions contain three adjustable parameters x,y,z. On the other hand the law of the superlattice extinctions is due to the fixed positions 12(*a*), 12(*b*) containing no parameter, which are occupied by the oxygen atoms of the normal fluorite lattice. To comply with these conditions, Belbeoch *et al.* concluded that the tetrahedra may only be relaxed without changing their tetrahedral geometry and this leads to a model where only displacements $\delta x=\delta y=\delta z=\varepsilon$ are possible but not $\delta x=\delta y\neq 0$ and $\delta z=0$.

The neutron diffraction results of Willis (1964) on the other hand give an indication of the relative numbers of oxygen atoms on fluorite lattice positions (O) and on two different interstitial positions O′ and O″ which correspond to displacements from the centre of an octahedral hole in $\langle 110\rangle$ and $\langle 111\rangle$ directions respectively. As mentioned in the literature, Willis (1965) found a distribution of oxygen in U_4O_9 of $U_1O_{1\cdot 77}O'_{0\cdot 31}O''_{0\cdot 14}$ which might indicate an ideal formula $U_{12}O_{21}O'_4O''_2$; that is, on the average there are in 3 UO_2 subcells 4 O atoms in position O′ and 2 O atoms in position O″ and the rest on normal lattice positions.

An important discrepancy between these findings and the model of Belbeoch *et al.* consists in the oxygen displacements. The model of Belbeoch *et al.* requires only displacements of type $\langle 111\rangle$ whereas the results of Willis indicate that both $\langle 110\rangle$ and $\langle 111\rangle$ type relaxations must occur in U_4O_9.

Other proposals published in the literature for oxygen positions obviously did not lead to agreement with the experimental superlattice reflexions.

So presently no definite model exists for the structure of U_4O_9 and the question arises whether other properties of U_4O_9 and UO_{2+x} might give an indication on the distribution of the oxygen ions. A first attempt in this direction has been made by Kingery (1965), which led him to propose the existence of molecular oxygen in UO_{2+x} and U_4O_9. In fact there are oxides which contain molecular oxygen like BaO_2, α-NaO_2, α-KO_2 and $CaO_2.8H_2O$ (Wells, 1962), and the bond length O–O is known in these cases. It is about 1·50 Å for the doubly charged negative molecule O_2^{2-}. If one accepts the local oxygen displacements found by Willis in the cubic uranium oxides no bond length O–O smaller than about 2 Å seems possible. Since also in U_3O_8 and UO_3 (Debets, 1966; Loopstra, 1963) no bond lengths O–O smaller than about 2·2 Å are found the hypothesis of Kingery appears doubtful even for a doubly charged molecule O_2^{2-}. So more experimental data are necessary.

4.3. *The transformation in* U_4O_{9-y} *and the* UO_2–U_4O_9 *phase diagram*

The striking difference of the diffraction patterns above and below the transformation temperature T_c indicates a change in entropy ΔS. Specific heat data of U_4O_{9-y} up to 700 °C obviously are not yet available, but one should expect an effect for C_p. Already on the basis of ΔS alone the transformation is certainly accompanied by a change in free enthalpy ΔG and therefore is of first order. Mostly such transformations are related to a change in volume, and the thermal expansion curves and lattice parameter *versus* temperature curves show a step at T_c. Yet this does not occur here, as the X-ray thermal expansion work of Ferguson & Street (1963) and of Belbeoch, Boivineau & Perio (1967) indicates.

In both investigations the lattice parameter *versus* temperature curves of U_4O_9 $a(T)$ are continuous between 100 °C and 1100 °C, only their slopes da/dT change around $T_c\sim 650$ °C. Both investigations are in good agreement. In the temperature region 200–650 °C they give a value $da/dT=6{\cdot}3\times 10^{-5}$ Å.deg^{-1} and in the region 650–1000 °C $8{\cdot}7\times 10^{-5}$ Å.deg^{-1} (Belbeoch, Boivineau & Perio, 1967) and $8{\cdot}4\times 10^{-5}$ Å.deg^{-1} (Ferguson & Street, 1963) can be deduced. In fact, Belbeoch, Boivineau & Perio (1967) have interpreted their results

* See *International Tables*.

by a continuous change of da/dT over the whole range 200–1100 °C, but it is at least equally well justified to draw two straight lines with a break in slope around 650 °C from their data.

If one compares the X-ray diffraction results published on U_4O_9 treated above 650 °C (Belbeoch, Laredo & Perio, 1964; Belbeoch, Boivineau & Perio, 1967) with our electron diffraction results, partial agreement is found with our observations: Belbeoch, Laredo & Perio (1964) found at 940 °C a disordered U_4O_{9-y} structure which should correspond to most of our electron diffraction results. On the other hand Belbeoch, Boivineau & Perio (1967) report on an U_4O_9 and U_4O_{9-y} which always shows superstructure lines above 650 °C. This behaviour was only found in one specimen out of eight in our investigation. So evidently both the ordered and the partly disordered U_4O_{9-y} can exist at $T > 650$ °C depending on yet unknown slightly different experimental conditions. Similar discrepancies occur also in the transformation near 70 °C (Naito, Ishii, Hamaguchi & Oshima, 1967; Belbeoch, Boivineau & Perio, 1967).

At present it is not possible to decide which type of high temperature U_4O_9 represents the true equilibrium. It is a well known fact that rather persistent metastable phases are possible in non-metallic systems (U_3O_7 phases, Fe–C system). So it seems justified to introduce the partly disordered U_4O_9 as a separate high temperature phase into a special version of the U–O diagram.

As explained in § 3.2.1 there is a strong indication that T_c increases with decreasing values of y in the composition formula U_4O_{9-y}. According to the results of Ferguson & Street (1963) the transformation took place around 500 °C for a specimen mixed with platinum powder in which some reduction occurred lowering the starting value O/U = 2·235, and a specimen without platinum powder, which must have kept its O/U = 2·235, transformed around 650 °C in qualitative agreement with the results presented in § 3.2.

Therefore an isotherm should be drawn in the phase diagram from a point near 500 °C and O/U ~ 2·23 to the left which then divides the phase boundary $UO_{2+x}/(UO_{2+x} + U_4O_{9-y})$ into a lower and an upper part. By this, the unusual shape of this phase boundary receives a very simple explanation and it has to be modified somewhat as shown in Fig. 10.

A strong indication for this modification can be found already in the literature from the E.M.F. work of Markin & Bones (Markin & Roberts, 1962; Markin & Bones, 1962). Their experimental points suggest that there should be a break in the course of the boundary near a point O/U ≃ 2·16, $T \simeq 560$ °C. In view of the uncertainties about an exact temperature of transforma-

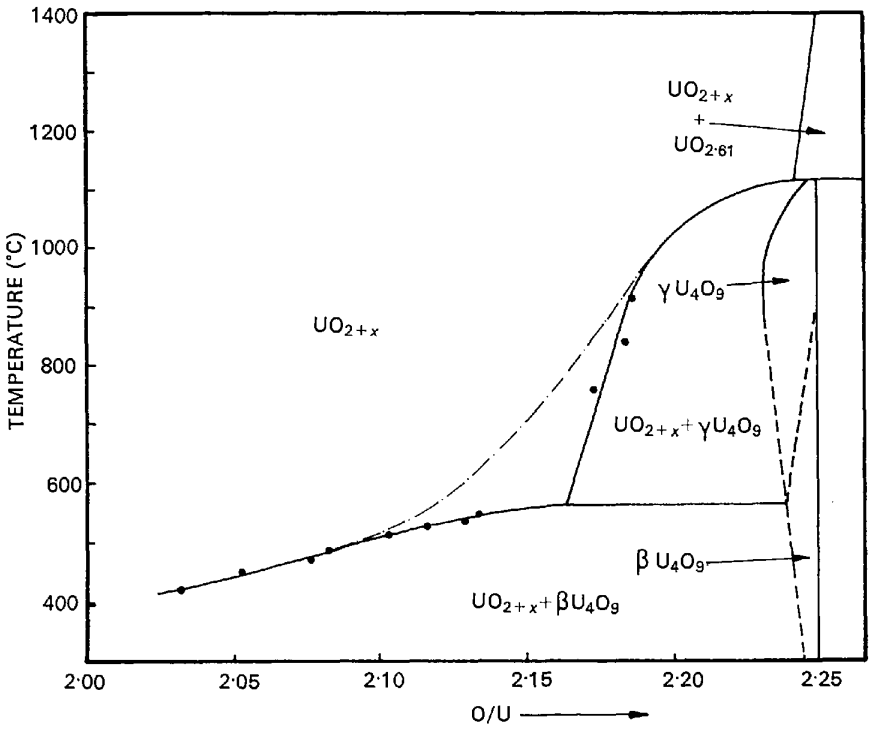

Fig. 10. Proposed modification of the U–O diagram taking account of the order–partial disorder transformation in U_4O_{9-y}. This version of the phase diagram probably does not replace the known phase diagram, but exists in addition to it. The experimental points of the phase boundary are taken from the work of Markin (Markin & Roberts, 1962). Three different modifications of U_4O_9 have been assumed; α at $T \leq 70$ °C, β at 80 °C $\leq T \leq T_c$, γ at $T_c \leq T \leq 1130$ °C.

tion the modified phase diagram has been based on the experimental points of Markin & Bones with T_c= 560 °C (Fig. 10).

4.4. *Crystallographic aspects of the transformation*

The relation between the low temperature diffraction spots of type $\mathbf{g}+\{112\}$ and the satellites at $T>T_c$ as indicated in Fig. 9 can be represented in the big U_4O_9 cell for each triangle of Fig. 9 by a relation equivalent to

$$[112]+[121]+[211] \rightarrow \tfrac{1}{3}[444] \qquad (1)$$

or

$$(112)+(121)+(211) \rightarrow \tfrac{1}{3}(444)\,. \qquad (1a)$$

The satellites of type $\mathbf{g}+\frac{1}{3}[444]$ are no more true superlattice reflexions since they occupy a finite volume in reciprocal space and this corresponds also to a finite reflecting volume in real space instead of a set of lattice planes.

Satellites around X-ray or electron diffraction spots may arise from different causes (Guinier, 1964):

(*a*) The regular spacing of antiphase boundaries in an ordered structure.

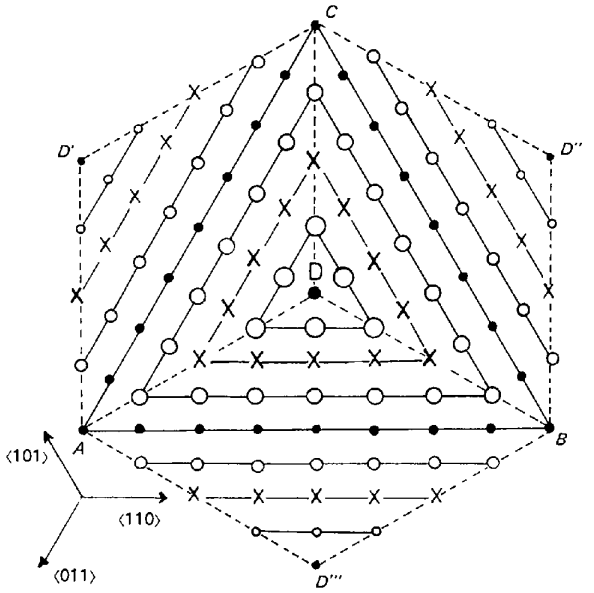

Fig. 11. Projection of the three planes (112) (121) and 211) on the plane (111); see relation (1). The (111) plane can be decomposed into these three planes giving a corrugated surface composed of triangular pyramids above and below the (111) plane. The base of each pyramid is determined by the distance $l=A-B$. Only the uranium atoms (small circles) and the oxygen atoms (open circles) of the basic UO_2 structure in the {112} planes are shown. Smaller circles indicate oxygen atoms below the (111) plane (plane of the drawing); bigger circles indicate oxygen atoms above this plane. Octahedral interstitial positions in the {112} planes are marked by crosses. In the U_4O_9 structure the excess oxygen atoms are located near these octahedral sites, but their detailed arrangement is still unknown. D is the top of the pyramid above the base ABC. The points D', D'' and D''' are the top points of inverted pyramids below the (111) plane of the drawing.

(*b*) The periodic variation of the spacing between a set of lattice planes.

(*c*) Quite generally the repeated occurrence of a lattice disturbance with a repeat vector $\mathbf{s}$ different from the reciprocal lattice vectors $\mathbf{g}$ which are parallel to $\mathbf{s}$.

In our case the satellites must have been produced by the relaxation of oxygen superlattice positions on {112} planes in such a manner that lattice disturbances with a repeat distance of

$$\frac{1}{D} \simeq \frac{1}{3a}[444] = \frac{1}{\sqrt{3}a_0} \qquad (2)$$

a_0 = lattice parameter of UO_2 unit cell

were created. Now there is a close relationship between the three {112} planes and the (111) plane of equation (1): Each (112) plane contains one of the three ⟨110⟩ directions, that is $[1\bar{1}0]$, $[10\bar{1}]$ and $[01\bar{1}]$, which are lying in the (111) plane, and also the three ⟨111⟩ directions besides the normal [111], that is $[\bar{1}11]$, $[1\bar{1}1]$ and $[11\bar{1}]$ are *in* the three {112} planes. In fact, the (111) plane can be decomposed into the three {112} planes whose normals are given by (1) and which then produce a corrugated surface composed of triangular pyramids one of which is drawn in Fig. 11 as a projection on the (111) plane.

Since according to the results of Willis, only displacements of oxygen in the directions ⟨111⟩ and ⟨110⟩ are possible in the UO_{2+x} and U_4O_9 structures, the close geometrical relationship (1) receives a physical meaning. The {112} and {111} planes are the only simple lattice planes of different type which both contain the same ⟨110⟩ directions and involve all possible ⟨111⟩ directions. So in the transformation the high temperature or low temperature structures can easily be interchanged by shifting oxygen ions only in ⟨111⟩ and ⟨110⟩ directions by very small distances.

By relation (1) the dimensions of the base of the triangular pyramids in the corrugated (111) planes of the crystal lattice are not yet fixed but this can be done by transforming the dimensions of the disc shaped satellites (Figs. 6 to 9) from reciprocal space into real space.

The lengths s_{tt} of the sides of the triangular discs are given by the vectors $[0\bar{1}1]$, $[1\bar{1}0]$ and $[10\bar{1}]$ if one takes the situation of the quenched structure of Fig. 8, *i.e.* if one neglects the diffuse intensity outside the triangle at high temperature. Transforming s_{tt} back to real space produces distances l along the three ⟨110⟩ directions of the (111) plane which are determined to a good approximation by the first zeros of the expression

$$(c/\pi x)\sin\frac{\pi x}{L} \text{ at } x=\pm L \text{ with}$$

$$l=2L;\ L=4a_0/\sqrt{2}\,. \qquad (3)$$

The distance $l=AB=BC=CA$ in Fig. 11 has been chosen according to (3) and it is equal to the diagonal of one face of the big U_4O_9 unit cell with $a=4a_0$. Each part of a {112} plane which represents a common face

to two inverted pyramids then contains the positions of 8 octahedral holes (Fig. 11).

At $T<T_c$ at least part of these holes should be occupied by excess oxygen atoms displaced from the centres of the holes by a vector $\Delta\mathbf{r}$ which lies *in* the corresponding {112} plane. At $T>T_c$ these oxygen atoms should be displaced by small amounts *out* of these planes creating crystal volumes containing disordered oxygen whose dimensions are roughly given by the pyramid *ABCD* in Fig. 11. The point *D* is the position of a uranium ion lying at $d=a_0/\sqrt{3}$ above the plane *ABC*, *i.e.* above the (111) plane. The mean distance of these disordered volumes in the [111] direction is given by relation (2).

4.5. *Conclusion*

Any model for the distribution of oxygen in U_4O_9 of space group $I\bar{4}3d$ should be in agreement with the three conditions (1) to (3), the directions and magnitudes of the oxygen displacements as deduced by Willis (1964) and the complete reciprocal lattice as given in Table 2.

These conditions might finally lead to an approach to the correct model of the structure from the point of view of lattice geometry. But it is not yet known if these conditions are sufficient to find this model without ambiguity.

References

AMELINCKX, S. (1964). *Direct Observation of Dislocations*. New York, London: Academic Press.

ANDRESEN, A. F. (1959). Enlarged symposium on reactor materials, Stockholm.

ARONSON, S. & BELLE, J. (1958). *J. Chem. Phys.* **29**, 151.

BELBEOCH, B., BOIVINEAU, J. C. & PERIO, P. (1967). *J. Phys. Chem. Solids*, **28**, 1267.

BELBEOCH, B., LAREDO, E. & PERIO, P. (1964). *J. Nucl. Mat.* **13**, 100.

BELBEOCH, B., PIEKARSKI, C. & PERIO, P. (1961). *Acta Cryst.* **14**, 837.

DEBETS, P. C. (1966). *Acta Cryst.* **21**, 589.

FERGUSON, I. F. & STREET, R. S. (1963). *Atomic Energy Research Establishment*, M 1192.

GOTOO, K., NOMURA, S. & NAITO, K. (1965). *J. Phys. Chem. Solids*, **26**, 1679.

GRØNVOLD, F. (1955). *J. Inorg. Nucl. Chem.* **1**, 357.

GUINIER, A. (1964). *Théorie et Technique de la Radiocrystallographie*. Paris.

HIRSCH, P., HOWIE, A., NICHOLSON, R. B., PASHLEY, D. W. & WHELAN, M. J. (1965). *Electron Microscopy of Thin Crystals*. Equation (8·23), p. 202. London: Butterworths.

KINGERY, W. D. (1965). CEA – S 5.

LEASK, M. J. M., ROBERTS, L. E. J., WALTER, A. J. & WOLF, W. P. (1963). *J. Chem. Soc.* p. 4788.

LOOPSTRA, B. O. (1963). RCN-INT-63-036.

MARKIN, T. L. & BONES, R. J. (1962). Atomic Energy Research Establishment, R 4042.

MARKIN, T. L. & ROBERTS, L. E. J. (1962). *Thermodynamics of nuclear materials*, p. 693. Vienna: IAEA.

NAITO, K., ISHII, T., HAMAGUCHI, Y. & OSHIMA, K. (1967). *Solid State Com.* **5**, 349.

NASU, S. (1966). *Jap. J. Appl. Phys.* **5**, 1001.

STEEB, S. (1961). *J. Nucl. Mat.* **3**, 235.

STEEB, S. & MITSCH, P. (1965). *J. Nucl. Mat.* **15**, 81.

WELLS, A. F. (1962). *Structural Inorganic Chemistry*, p. 406. Oxford Univ. Press.

WILLIS, B. T. M. (1963). *Nature, Lond.* **197**, 755.

WILLIS, B. T. M. (1964). *J. physique* **25**, 431.

WILLIS, B. T. M. (1965). Personal communication to KINGERY, W. D. (1965).

Acta Cryst. (1968). A**24**, 666

Création de Nouveaux Champs d'Ondes Dus à la Présence d'un Objet Diffractant à l'Intérieur d'un Cristal Parfait. I. Cas d'une Fente

PAR F. BALIBAR

Laboratoire de Minéralogie-Cristallographie, Sorbonne, Paris 5e, France

(*Reçu le* 20 *mars* 1968)

Green's functions are used to calculate the amplitude distribution on the exit surface of a perfect crystal in which a wave field, travelling according to the dynamical theory (Laue case), is diffracted by a slit lying inside the crystal. It is shown that this diffraction process induces interbranch scattering and that two wave fields are excited, belonging to both branches of the surface of dispersion. The fine structure of both beams is found to be identical with that obtained by Takagi's theory when the slit lies on the entrance surface of the crystal.

Introduction

La méthode des topographies aux rayons X par transmission permet d'obtenir des images de dislocations dans des cristaux presque parfaits. L'étude du contraste de ces images a fait l'objet de plusieurs travaux et il est maintenant possible de donner une interprétation des différentes parties qui constituent ces images.